Towards building 3D individual models from MRI segmentation and tractography to enhance pediatric surgery planning of pelvic tumors and malformations

Cécile Olivia MULLER, Alessio VIRZÍ, Jean-Baptiste MARRET, Eva MILLE, Laureline BERTELOOT, David GREVENT, Thomas BLANC, Nicolas GARCELON, Isabelle BUFFET, Elisabeth HULLIER AMMARD, Pietro GORI, Nathalie BODDAERT, Isabelle BLOCH, Sabine SARNACKI

IMAG2 Laboratory, Imagine Institute, Paris, France
Data science platform, Imagine Institute, Paris
Clinical research department, Imagine Institute, Paris, France
Pediatric surgery and radiology departments, Necker Hospital, APHP, Paris, France
LTCI, Télécom ParisTech, Université Paris-Saclay, Paris, France
Contact: cecile.muller@aphp.fr

Patient specific 3D modeling is the first step towards image-guided surgery, which is the next revolution in surgical care. Pediatric patients presenting rare tumors and malformations should benefit from these latest technological innovation, to improve surgical precision. Individual patient's models can be derived from imaging data. The pelvis region, being located at the crossroad of the urinary, digestive and genital channels with important vascular and nervous structures, is particularly difficult to imagine in 3D. We report our preliminary results in computing patient-specific 3D models from MRI of pelvic tumors or malformations in children. Imaging of the peripheral nervous network of the pelvis and its integration in the 3D model of the patient were also studied.

1 Patients and MRI

1.1 Patients

Since 2016, patients from 3 months to 18 years of age presenting pelvic tumors or malformations were included in the study, after ethic board committee agreement. Clinical and radiological data, surgical photos and videos were collected in a interactive and prospective database. Until now, 65 patients were included in the study: 28 tumors, 34 malformations and 3 controls (Table 1).

Table 1: *Patients' pathologies.*

Tumors	28	Malformations	34
Ovarian tumor	12	Anorectal malformation	27
Sacro-coccygeal teratoma	6	Urogenital malformation	5
Urogenital rhabdomyosarcoma	4	Sacro-coccygeal dimple	2
Neurofibroma (NF1)	3		
Ganglioneuroma	2		
Kystic lymphangioma	1		

1.2 Pelvic MRI acquisition

Radiological examination was performed on a 3Tesla MRI with a standard protocol as done in clinical routine and two additional sequences required for 3D modeling (3D T2 acquisition) and tractography (axial diffusion tensor) (Table 2).

All patients under 5 years of age received sedation with Phenobarbital. No general anesthesia was required. Glucagon injection and respiratory trigger were also used to avoid artifacts.

Table 2: *MRI acquisition protocol (TR, FA and TE stand for repetition time, flip angle, and echo time, respectively).*

Sequence	Plan	TR (ms)	FA (°)	TE (ms)	Vox.Size (mm)
Ax T2	Ax	11573	120	95	0.47x0.47x4.4
Sag T2	Sag	8544	140	118	0.47x0.47x4.8
Ax T1	Ax	655	160	8.7	0.47x0.47x4.5
Ax T1 FS Gado	Ax	724	160	7	0.66x0.66x1.2
Diffusion	Ax	6000	90	60	1.02x1.02x5
Cube T2	Coro	2609	90	68	0.62x0.62x0.6
Water Lava HR T1	Ax	4	12	1.7	0.55x0.55x1
Diffusion Tensor	Ax	6179	90	53	1.25x1.25x3.5

Complementary parameters of diffusion tensor were: direction number = 25; b = 600.

2 Image processing and analysis

2.1 3D segmentation

Benchmarking of available softwares for image processing according to seven main criteria (automation degree, segmentation time, usability, 3D visualization quality, image registration, tractography and potential plugins) allowed us to identify 3D Slicer [4] for the development of compatible in-house semi-automatic plugins [18] to perform 3D patient specific models.

A method based on CT age-matched templates was used to reduce the segmentation time dedicated to the pelvic bones, which was hence reduced from 90 to 5 minutes on average. Plugins for the bladder, vessels and rectum are under development.

An entire 3D patient specific model was computed for 35 patients (Figure 1), using the developed semi-automatic plugin for the pelvic bones and manual segmentation for the other organs: digestive, genito-urinary, vessels and muscles. After a learning stage using 3D Slicer, the global segmentation time dropped to 7 hours on average, including tractography.

2.2 Tractography

The imaging of the peripheral nervous system has recently been made feasible thanks to the advances of diffusion MR sequences and of tractography algorithms, providing 3D images of nerve fibers.

Regarding the integration of peripheral nervous anatomy in the patient specific 3D model, a comparison of three tractography softwares (AW-Server, OLEA Sphere®, 3D Slicer) was performed in 4 patients. The visual results were quite similar (Figure 2). A quantitative comparison using 10 points of the pelvis nervous network (S2, S3, S4, hypogastric plexus and pudendal nerve (left and right)) according to three criteria of analysis (mean number of fibers, mean fractional anisotropy and mean radial diffusivity) is in progress.

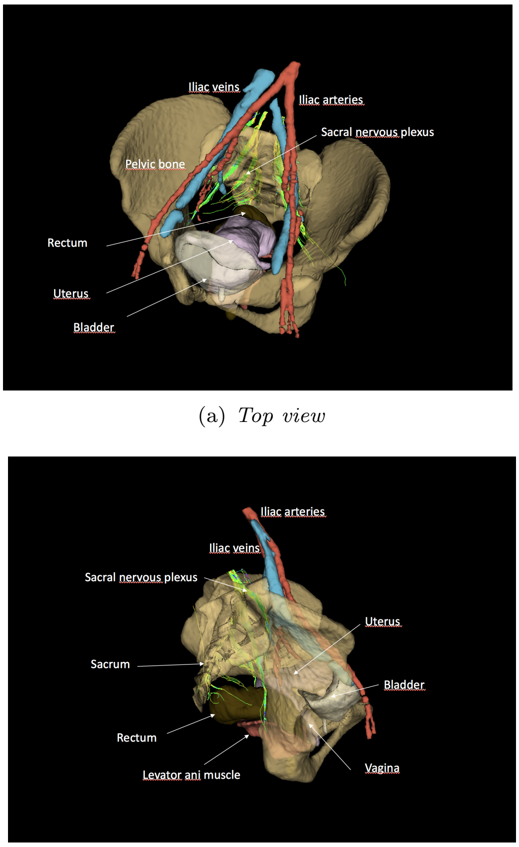

(a) *Top view*

(b) *Profile view*

Figure 1: *Example of 3D patient-specific model of a control 15 years old girl (visualization using 3D slicer).*

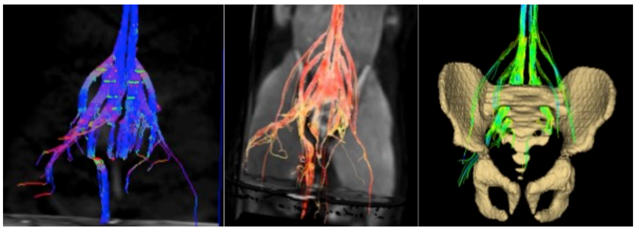

Figure 2: *Example of pelvic tractography of a 4 years old child with rectal stenosis, using OLEA Sphere, AW-Server and 3D Slicer (from left to right).*

3 Conclusion

These preliminary results are the first steps towards computing semi-automatic 3D individual models from MRI, including the peripheral nervous system network, for pediatric malformations and tumors of the pelvis. Beside the improvement of the preoperative surgical strategy, as demonstrated already on few cases, and in the future its obvious utility for image-guided surgery, this computational anatomy will allow for comparison studies between imaging and function, and between endophenotype and genotype in rare pediatric tumors and malformations.

References

[1] Azagury DE, Dua MM, Barrese JC, Henderson JM, Buchs NC, Ris F, Cloyd JM, Martinie JB, Razzaque S, Nicolau S, Soler L, Marescaux J, Visser BC (2015) Image-guided surgery. Curr Probl Surg 52:476–520.

[2] Bertrand, M. M., Macri, F., Mazars, R., Droupy, S., Beregi, J. P., and Prudhomme, M. (2014). MRI-based 3D pelvic autonomous innervation: a first step towards image-guided pelvic surgery. European Radiology, 24(8), 1989–1997.

[3] Cauley, K. A. and Filippi, C. G. (2013). Diffusion-Tensor Imaging of Small Nerve Bundles: Cranial Nerves, Peripheral Nerves, Distal Spinal Cord, and Lumbar Nerve Roots Clinical Applications. American Journal of Roentgenology, 201(2), W326–W335.

[4] Fedorov A., Beichel R., Kalpathy-Cramer J., Finet J., Fillion-Robin J-C., Pujol S., Bauer C., Jennings D., Fennessy F.M., Sonka M., Buatti J., Aylward S.R., Miller J.V., Pieper S., Kikinis R. 3D Slicer as an Image Computing Platform for the Quantitative Imaging Network. Magn Reson Imaging. 2012 Nov;30(9):1323-41.

[5] Ferrari V, Carbone M, Cappelli C, Boni L, Melfi F, Ferrari M, Mosca F, Pietrabissa A (2012) Value of multidetector computed tomography image segmentation for preoperative planning in general surgery. Surg Endosc 26:616626.

[6] Finley, D. S., Ellingson, B. M., Natarajan, S., Zaw, T. M., Raman, S. S., Schulam, P., et al. (2012). Diffusion Tensor Magnetic Resonance Tractography of the Prostate: Feasibility for Mapping Periprostatic Fibers. Url, 80(1), 219–223.

[7] Haak D, Page C-E, Deserno TM (2016) A Survey of DICOM Viewer Software to Integrate Clinical Research and Medical Imaging. J Digit Imaging 29:206215. doi: 10.1007/s10278-015- 9833-1

[8] Haakma, W., Dik, P., Haken, ten, B., Froeling, M., Nievelstein, R. A. J., Cuppen, I., et al. (2014). New Technology and Techniques Diffusion Tensor Magnetic Resonance Imaging and Fiber Tractography of the Sacral Plexus in Children with Spina Bifida. Juro, 192(3), 927–933.

[9] Kitajima, K., Takahashi, S., Ueno, Y., Miyake, H., Fujisawa, M. and Sugimura, K. (2014). Visualization of periprostatic nerve fibers before and after radical prostatectomy using diffusion tensor magnetic resonance imaging with tractography. Journal of Clinical Imaging, 38(3), 30–306.

[10] Lo Presti G, Carbone M, Ciriaci D, Aramini D, Ferrari M, Ferrari V (2015) Assessment of DICOM Viewers Capable of Loading Patient- specific 3D Models Obtained by Different Segmentation Platforms in the Operating Room. J Digit Imaging 28:518527.

[11] Manganaro, L., Porpora, M. G., Vinci, V., Bernardo, S., Lodise, P., Sollazzo, P., et al. (2013). Diffusion tensor imaging and tractography to evaluate sacral nerve root abnormalities in endometriosis-related pain: A pilot study. European Radiology, 24(1), 95–101.

[12] Marescaux, J. and Diana, M. (2014). Inventing the Future of Surgery. World Journal of Surgery, 39(3), 615–622.

[13] Marescaux J and Diana M. (2015) Next step in minimally invasive surgery: hybrid image-guided surgery., J Ped Surg 50(1), 30–36.

[14] Megali G, Ferrari V, Freschi C, Morabito B, Cavallo F, Turini G, Troia E, Cappelli C, Pietrabissa A, Tonet O, Cuschieri A, Dario P, Mosca F (2008) EndoCAS navigator platform: a common platform for computer and robotic assistance in minimally invasive surgery. Int J Med Robot Comput Assist Surg MRCAS 4:242–251.

[15] Peters TM (2006) Image-guidance for surgical procedures. Phys Med Biol 51:R505–540.

[16] Soler L, Nicolau N, Fasquel JB, Agnus V, Charnoz A, Hostettler A, Moreau J, Forest C, Mutter D, Marescaux J. (ISBI 2008). Virtual Reality and Augmented Reality applied to Laparoscopic and NOTES procedures

[17] Van der Jagt, P. K. N., Dik, P., Froeling, M., Kwee, T. C., Nievelstein, R. A. J., Haken, ten, B. and Leemans, A. (2012). Architectural configuration and microstructural properties of the sacral plexus: A diffusion tensor MRI and fiber tractography study. NeuroImage, 62(3), 1792–1799.

[18] Virzi A., Muller C.O., Marret J–B., Berteloot L., Boddaert N., Sarnacki S. and Bloch I. (2017). A new method based on template registration and deformable models for pelvic bones semi-automatic segmentation in pediatric MRI. IEEE 14th International Symposium on Biomedical Imaging (ISBI), 323–326.

[19] Wada, K., Hashimoto, T., Miyagi, R., Sakai, T. and Sairyo, K. (2016). Diffusion tensor imaging and tractography of the sciatic nerve: assessment of fractional anisotropy and apparent diffusion coefficient values relative to the piriformis muscle, a preliminary study. Skeletal Radiology, 1–6.